# Shell-driven Fission across the Nuclear Chart

*D.J.* Hinde[1,*], *J.* Buete[1], *B.M.A.* Swinton-Bland[1], *K.J.* Cook[1], *M.* Dasgupta[1], *A.C.* Berriman[1], *D.Y.* Jeung[1], *K.* Banerjee[1,**], *L.T.* Bezzina[1,***], *I.P.* Carter[1,****], *C.* Sengupta[1,†], *C.* Simenel[2], and *E.C.* Simpson[1]

[1]Department of Nuclear Physics and Accelerator Applications, Research School of Physics, Australian National University, Canberra, ACT 2601, Australia
[2]Department of Fundamental and Theoretical Physics, Research School of Physics, Australian National University, Canberra, ACT 2601, Australia

**Abstract.** Results are presented from a broad, systematic study of heavy-ion induced fusion-fission mass distributions carried out at the Australian National University, covering a significant part of the chart of the nuclides. Fission characteristics of isotopes of every even-Z compound nucleus ($Z_{CN}$) from $^{164}_{64}$Gd to $^{212}_{90}$Th were measured. Systematic evidence of shell-driven structure is present in every fission mass distribution. The changing shape of the heavy-ion fission mass distributions with $Z_{CN}$ is visualised through the residuals from single Gaussian fits. These results are consistent with quantitative fitting of the measured 2-D mass and total kinetic energy spectra using multiple components. Both approaches demonstrate that fragment proton shell gaps around $Z_{FF}$ = 34, 36 and around $Z_{FF}$ = 44, 46 are major drivers of fission mass distributions for nuclei below the actinide region. Significantly, the mass distributions show enhanced yields at mass-symmetry for values of $Z_{CN}$ equal to two times these favoured $Z_{FF}$ values. The same shell gaps that favour mass-asymmetric fission thus also affect mass distributions at and near mass-symmetry. For all systems, a second more mass-asymmetric fission mode is required to fit the fission mass distributions. If driven by a single shell gap, it appears to be in the light fragment, around $Z_{FF}$ ~28,30 or possibly $N_{FF}$ ~44.

## 1 Introduction

Fission products were first identified unambiguously by Hahn and Strassmann [1], following neutron bombardment of uranium, observing the production of radioactive barium nuclei. This led Meitner and Frisch to come up with the revolutionary idea [2] that heavy nuclei could split into two large fragments, coining the term "nuclear fission". The barium fission fragments identified as the first evidence of fission correspond to a mass-asymmetric split of U (Z=92) into Ba (Z=56) and Kr (Z=36). This is counter to the liquid drop model (LDM) of fission that was soon developed to explain the mechanism by which fission can arise. The LDM favours mass-symmetric splits. Fig.1(a) illustrates a calculated LDM potential energy surface, showing that the lowest barrier (saddle-point) between the ground-state and fission is mass-symmetric. It was realised that structure on the potential energy surface (PES) is generated by the quantum-mechanical single-particle level structure of the nascent fission fragments, as illustrated in Fig.1(b). This can result in favouring of mass-asymmetric fission.

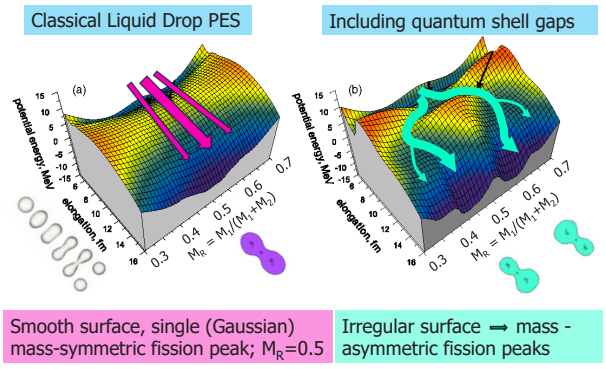


**Figure 1.** Calculated fission potential energy surfaces (PES) without (a) and with (b) the effects of single particle shell gaps. The mass-ratio $M_R$ is the ratio of one fragment mass to the total mass of the fissioning system, and is the quantity many experimental techniques determine. The probabilities of fission trajectories, following the lowest saddle-points and valleys on the PES, are indicated by the width of the arrows. Adapted from Ref. [3].

Actinide nuclei have been found to fission preferentially mass-asymmetrically at low excitation energy ($E_x$), as illustrated in Fig.2(a) from a recent measurement of spontaneous fission of $^{248}$Cm [4]. With increasing $E_x$, mass-symmetric yields almost always increase (see Ref. [4] for an in-depth analysis). This is illustrated in Fig.2(a), which shows the fission $M_R$ distribution for the

*e-mail: david.hinde@anu.edu.au
**Permanent address: Variable Energy Cyclotron Centre, 1/AF, Bidhan Nagar, Kolkata 700064, India.
***Present address: Department of Physics, ETH Zurich, Switzerland
****Present address: DST Group, Canberra, Australia
†Present address: Image X Institute, Sydney School of Health Sciences, University of Sydney, Sydney, Australia

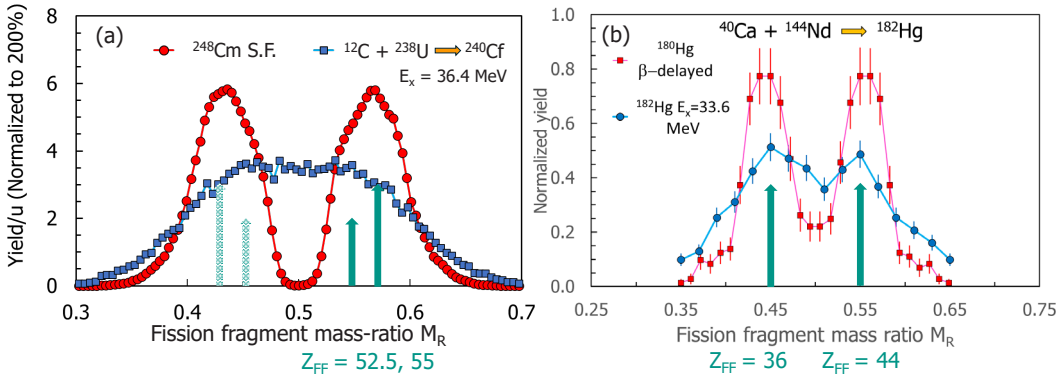


**Figure 2.** (a) Normalized mass-ratio yields for two neighbouring actinide nuclides. The spontaneous fission (S.F.) arises from the ground-state, and here the yield at mass-symmetry is negligible [4]. The fusion-fission reaction [5, 6] populates much higher excitation energy $E_x$, and this is understood to be the reason for the increased yield at symmetry, and the attenuated character of the structure. (b) A similar comparison is shown for two isotopes of Hg [7, 8], displaying very similar behaviour, though with slightly more structure apparent in the heavy-ion reaction than in (a). Proton numbers $Z_{FF}$ that have been associated with the mass-asymmetric structures are indicated (see text).

neighbouring nuclide $^{240}$Cf formed at $E_x$=36 MeV. Fits to actinide fission charge distributions [9] indicated that two fission "modes", associated with heavy fragment charges $Z_{FF}$ averaging 52.5 and 55 could reproduce the major systematic behaviour of mass-asymmetric actinide fission.

## 2 Mass-asymmetric fission of Hg nuclides

Nuclides lighter than the actinides have increasingly higher fission barriers, as a result of the smaller value of the Coulomb term (proportional to $Z^2$) in the mass formula. Thus they generally undergo fission only at higher $E_x$. These mainly have mass distributions peaked at mass-symmetry (though there are exceptions, see Refs.[10, 11]). The seminal work of Andreyev *et al.* [7] marked a major breakthrough, with the observation of dominant mass-asymmetric fission of $^{180}$Hg from low $E_x$. This gave the first indication that quantum level structure can very significantly influence fission of nuclides lighter than lead. This distribution in shown in red in Fig.2(b).

Subsequently, measurements were made of heavy-ion induced fusion-fission forming compound nuclei (CN) of the same or neighbouring neutron-deficient Hg nuclides. These fusion reactions limit the lowest $E_x$ above the ground-state to be > 30 MeV. Nevertheless, the measurements showed [8, 15] that evidence of mass-asymmetric fission persists, as seen in Fig.2(b), despite the expectation that shell effects should be attenuated at higher $E_x$.

The Hg region fission mass distributions showed peaks that may be associated with proton numbers $Z_{FF} \sim 36$ or 44 (or possibly both), depending on whether shell gap(s) in the light or the heavy fragment are dominant (or both). These values are quite different from the proton numbers believed to be dominant in actinide fission.

## 3 Systematics of sub-actinide fission mass distributions

As in the actinides [9], measurements for a long sequence of nuclides are important to achieve a systematic understanding of fission mass distributions. It is useful to study a sequence with similar compound nucleus N/Z. It is a good approximation that the N/Z of the fragments is that of the compound nucleus (the unchanged charge division – UCD – approximation). Thus fission fragments favoured by a particular shell-gap (associated with certain proton or neutron numbers) *will* be produced for each fissioning nucleus. However, they will occur at a different mass-asymmetry depending on the fissioning nucleus mass. Thus the structure in each mass distribution should have a quantitative relationship with all the others.

Measurements were performed at the Heavy-Ion Accelerator Facility at the Australian National University us-

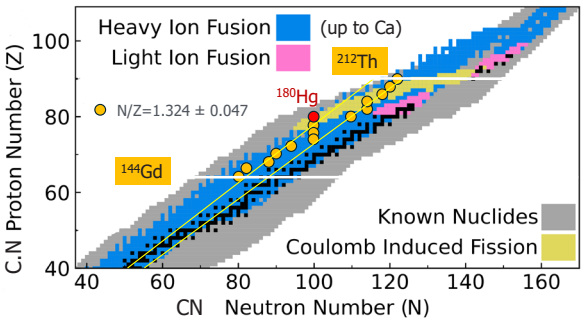


**Figure 3.** Chart of the Nuclides showing stable nuclides (black squares), nuclides whose fission has been studied by Coulomb excitation of relativistic radioactive beams [12, 13] (yellow), and nuclides accessible by fusion-fission using stable projectile nuclides up to Ca and stable target nuclides (blue). The nuclides whose fission was measured in the work of Buete *et al.* [14] are shown by yellow circles, with the lower and upper boundaries in Z indicated by the horizontal white lines.

ing the CUBE fission spectrometer. Pulsed beams of $^{32,34}$S and $^{16}$O were delivered onto isotopically-enriched thin targets ranging from $^{112}$Cd to $^{180}$W, having areal densities from 7 to 140 $\mu$g cm$^2$. Reactions were chosen to produce a series of neutron-deficient isotopes centred around N/Z = 1.324, with standard deviation 0.047. Beam energies were selected to minimise $E_x$ whilst having sufficient fission cross-section to aim for 50,000 fission events. This resulted in $E_x$ values from 41 – 70 MeV.

The compound nuclei produced are indicated by yellow circles in Fig.3, comprising an isotope of each even-Z element extending from Gd ($Z_{CN}$=64) to Th ($Z_{CN}$=90). The absence of fast quasifission was demonstrated by the mass-ratio centroids remaining at 0.5 as a function of detection angle. Furthermore, a systematic classification based on average fissility [16] suggests that slow quasifission should be negligible except for the heaviest of these reactions [17–21]. Together with the relatively low values of c.m. energy with respect to the capture barrier [22], the mass spectra should be representative of fusion-fission, with insignificant "memory" of the initial mass-asymmetry of the projectile and target.

As described in detail in Section 5, the experimental data were ultimately fitted with 2-D Gaussians associated with the characteristic mass and TKE of the constituent fission modes. Before this analysis, a simple method to visualise the systematic behaviour of the mass distributions was applied.

## 4 Residuals from single Gaussian fits to the mass-ratio distributions

The measured mass-ratio distribution for fission of $^{178}$Pt is shown in the upper panel of Fig. 4. It reveals a double-peaked structure indicative of a significant contribution from a mass-asymmetric fission mode. The best-fitting single Gaussian is shown in orange. The difference between the experimental data and the fit (the residuals spectrum) is shown below. It displays the expected shape, having a well-defined dip at mass-symmetry, and two positive peaks displaced equally from $M_R$ = 0.5.

The experimental data, fits, and residuals are shown for the range of measured systems from $^{144}$Gd to $^{212}$Th in Fig. 5. Consider firstly the right-hand columns, from $^{178}$Pt to $^{212}$Th. The mass-asymmetric positive residual peaks become weaker with increasing $Z_{CN}$ and transition to a peak at mass-symmetry for Rn, Ra and Th ($Z_{CN}$ = 86 to 90). If the mass-asymmetry for $^{178}$Pt resulted from a shell gap at $Z_{FF}$ = 44, this shell gap should favour mass-symmetric fission around $Z_{CN}$=88, which seems to be the case.

Consider now the left-hand columns, transitioning down in $Z_{CN}$ from $^{176}$Os ($Z_{CN}$ = 76). A peak in the residuals at symmetry is already seen for $Z_{CN}$ = 72 to 68. This suggests that shell gaps around $Z_{FF}$ = 36, 34 play a role here. These should also contribute to the mass-asymmetric structure in the fission mass distributions in the Pt region. By $Z_{CN}$ = 66 and 64, a mass-asymmetric peak reappears, as would be expected for this scenario.

The trends of the structure seen in the mass distribution residual are highlighted by the near-vertical long green lines. Shell gaps at Z~34,36 and Z~44 seem to contribute jointly to the strong mass-asymmetric fission clearly seen in the Os, Pt, Hg isotopes. They contribute in both fragments to mass-symmetric fission for the Er, Yb, Hf and Rn, Ra, Th isotopes respectively. It is important to emphasise that this (qualitative) conclusion may not be universal, being valid over the (narrow) range of N/Z values investigated in this study.

Taking the analysis of the experimental results to a more quantitative level, 2-D fitting of multiple modes was carried out, and the results compared with the above qualitative conclusions, as described in Section 5 below.

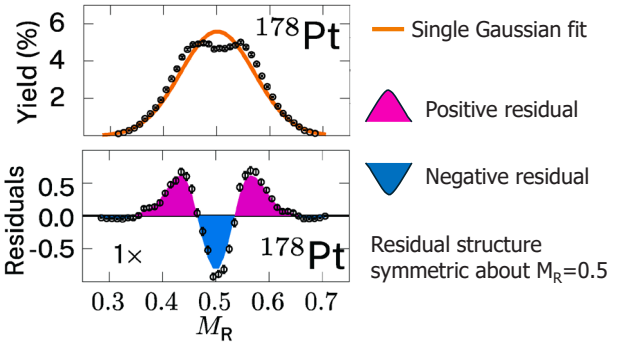


**Figure 4.** Heavy-ion induced fission mass-ratio distribution for $^{178}$Pt, with the single Gaussian best-fit in orange. Below is the distribution of residuals, showing the characteristic structure associated with a mass-asymmetric fission component. As expected, for fusion-fission the residuals are symmetric about $M_R$ = 0.5.

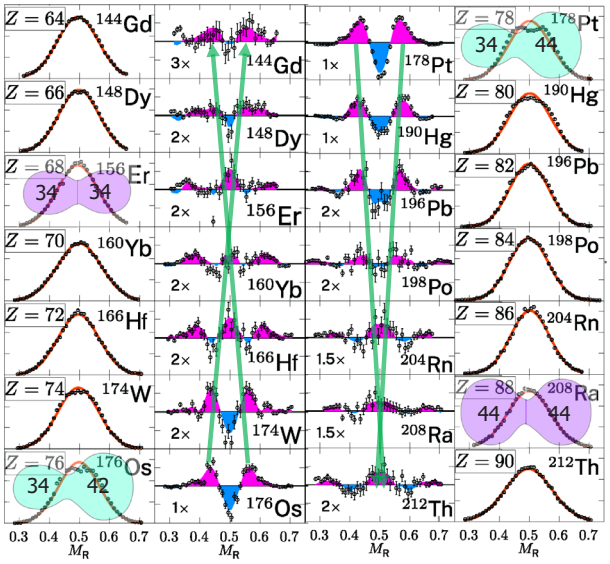


**Figure 5.** Systematics of the mass-ratio spectra and the residuals from single Gaussian fits for heavy-ion induced fusion-fission of every even-Z element from Gd (Z=64) to Th (Z=90). The residuals show a consistent trend from being peaked at $M_R$=0.5 for Th, to well-defined peaks at mass-asymmetry around Pt, then back to symmetry for systems centred on Yb, finally returning to mass asymmetry for Gd. The green lines highlight these trends. Adapted from Ref. [14].

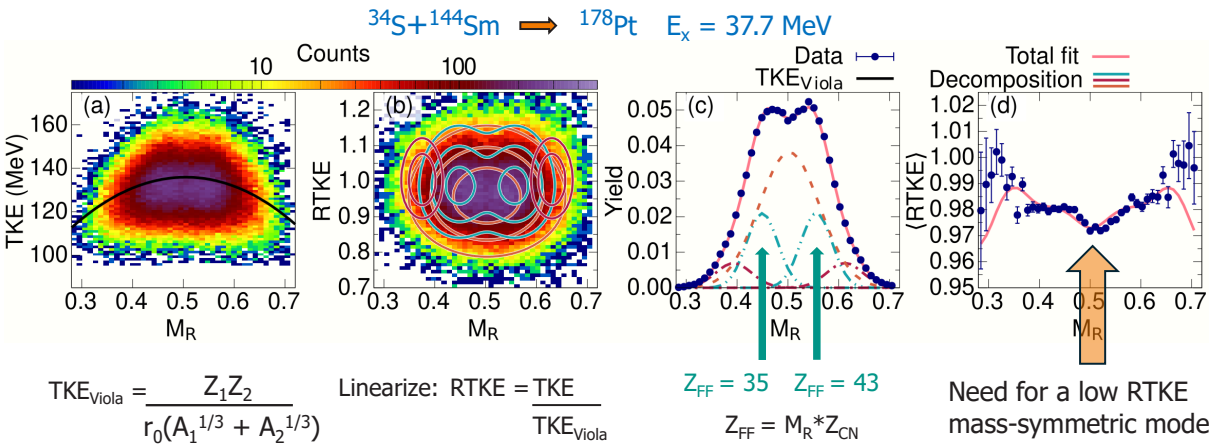


**Figure 6.** Measured fission characteristics [23] for heavy-ion induced fission of $^{178}$Pt. (a) shows mass-ratio $M_R$ vs. TKE, and (b) the linearized quantity RTKE (as defined in the figure) vs. $M_R$. The 2-D fitted components are indicated using the colour scale at top right. The total mass spectrum is given in (c), with the components of the best fit. The mean RTKE as a function of $M_R$ is shown in (d), with the feature at $M_R$=0.5 indicating the need for a mass-symmetric mode with low RTKE. Adapted from Refs. [23, 24].

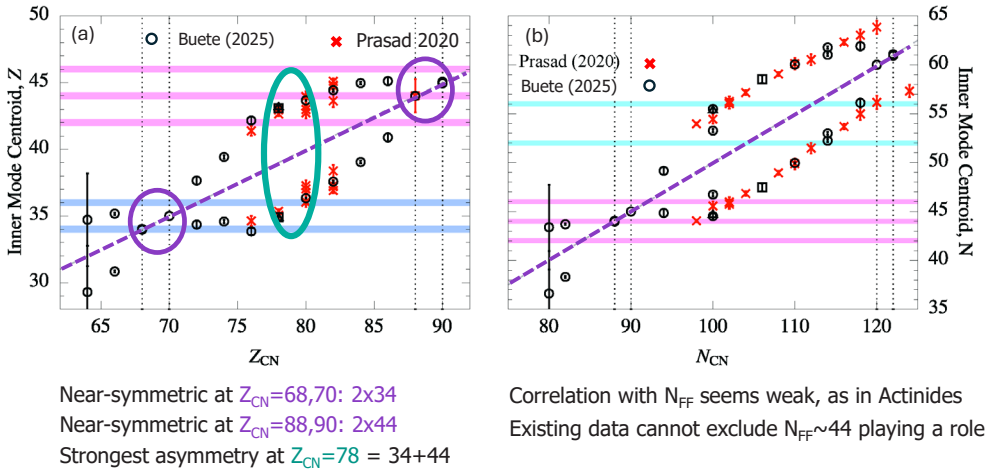


**Figure 7.** Systematics of inner mass-asymmetic peak centroids. Symmetric mass-splits are indicated by the dashed purple lines. Expected shell gaps [25, 26] are indicated by horizontal coloured lines. (a) shows the values of $Z_{FF}$ (determined using the UCD approximation) as a function of $Z_{CN}$, with green and purple highlighted regions discussed in the text. (b) is analagous to (a), but for neutron numbers. Data from Refs. [14, 27], figure adapted from Ref. [14].

## 5 Fitting of Mass-TKE distributions to extract shell structure

This work [14] followed the approach described by Swinton-Bland and Buete *et al.* [23] in the analysis of fission of $^{178}$Pt. Fig. 6(a) shows the experimental fission mass-ratio vs. fission Total Kinetic Energy (TKE) spectrum. The black curve shows the expected dependence of TKE on $M_R$ based on the charge product and sizes of the two fragments, with $r_0$ adjusted to match the empirical Viola TKE systematics [28]. Fitting the data is complicated by this expected relationship. Fitting can be simplified by linearizing the data, dividing the TKE at each point in the 2-D spectrum by the Viola expectation [21]. This gives the relative TKE (RTKE) vs. $M_R$ spectrum as shown in Fig. 6(b). In fitting, each asymmetric mode is represented by a 2-D Gaussian, characterised by its displacement from mass-symmetry, RTKE value, and respective Gaussian widths. A mass-symmetric mode may also be included.

Good reproduction of the experimental spectra could be achieved with two mass-asymmetric modes, and a mass-symmetric mode, each with different central RTKE, exemplified for $^{178}$Pt in Fig. 5(b). The projections of the yields and mean RTKE onto $M_R$ are shown in Fig. 5(c) and (d) respectively, for the total fit (pink), and also in (c) for the components. The significant dip in RTKE near $M_R$=0.5 can only be reproduced with a low RTKE mass-symmetric mode.

This procedure was repeated for each compound nucleus, obtaining the $M_R$ centroids of the two mass-asymmetric modes. These were converted to the associated proton numbers of the fission modes ($Z_{FF}$), or the neutron numbers ($N_{FF}$) using the UCD approximation. Thus $Z_{FF}$=$M_R$.$Z_{CN}$ and $N_{FF}$=$M_R$.$N_{CN}$. The use of other

approaches to estimate these numbers [14] would change the determined centroid positions by less than 0.5 protons, which is below the precision expected from the fitting process.

The inner mode centroids extracted in this way are shown by open black circles in the left panel of Fig. 7, plotted as a function of $Z_{CN}$. The results show a very systematic behaviour, correlated with $Z_{FF}$~34,36 for the lower $Z_{CN}$, and with $Z_{FF}$~44 for the higher $Z_{CN}$. The green ellipse indicates where the strongest evidence of mass-asymmetric fission is seen, corresponding to both fragments having favoured $Z_{FF}$ values. Where the inner mode approaches the mass-symmetric mode (purple circles), the unconstrained parameters of the symmetric and inner mass-asymmetric modes in the fit can play off against each other, leading to larger uncertainties, as indicated. The lower statistics and more limited fitting environment of the work of Prasad et al. [27] (red crosses) are in good agreement.

The observed structure in the fission characteristics could alternatively be correlated with neutron shell gaps in the nascent fission fragments. Fits to $^{178}$Pt and $^{184}$Pt from this data set [14] both return $Z_{FF}$ = 35 for the inner asymmetric mode However, $N_{FF}$ moves from 44 to 47. Therefore, it was concluded [14] for Pt, proton shell gaps are responsible.

Over the whole data set [14], the extracted values of $N_{FF}$ are shown as a function of $N_{CN}$ in the right hand panel of Fig. 7. Also shown (red symbols) are the results from Ref. [27], where a wide range of N/Z was specifically investigated for isotopes of Os to Pb. All data show no evidence for any favoured $N_{CN}$ above $N_{CN}$ = 98. Measurements for different isotopes of lighter elements would be necessary to determine whether any neutron shell gap near $N_{FF}$ = 44 might be playing a role.

For all systems, a second more mass-asymmetric fission mode is required to fit the fission mass distributions. If driven by a single shell gap, it appears to be in the light fragment, around $Z_{FF}$ ~28,30 or possibly $N_{FF}$ ~44. Further measurements are needed to better define this feature.

## 6 Summary

Structure has been found universally in fission mass and TKE distributions following heavy-ion fusion reactions, in a systematic series of measurements forming an isotope of every even-Z element from Gd ($Z_{CN}$ = 64) to Th ($Z_{CN}$ = 90).

Independent fitting of the data for each compound nucleus showed consistent trends in the location of structures, consistent with the influence of proton shell gaps at both $Z_{FF}$~ 34,36 and $Z_{FF}$~ 44. The wide coverage in $Z_{CN}$ showed experimentally that the shell gaps affect fission characteristics not only for asymmetric mass-splits, as in the actinides, but also at mass-symmetry.

To extract the maximum information from experiments, several aspects should be considered: (i) measurements should aim for > $10^5$ events in a mass-TKE matrix; (ii) mirroring the distributions about mass-symmetry can obscure experimental issues, and even generate spurious structure, so is not recommended; (iii) because of the large number of fit parameters when multiple fission modes are present, a single gradient-descent chi-squared fit is unlikely to find the lowest minimum, or provide the correct experimental uncertainty. A detailed exposition on many of these points is given in the PhD thesis of J. Buete [29].

## Acknowledgments

The authors acknowledge the Australian Research Council for support through DECRA Fellowship DE230100197 and Discovery grants DP170102318, DP190101442, DP190100256, DP200100601, and DP230101028. Financial support for accelerator operations was provided by the Australian National Collaborative Research Infrastructure Strategy (NCRIS) through the Heavy Ion Accelerators (HIA) project.

## References

[1] O. Hahn, F. Strassmann, About the evidence and the behavior in uranium radiation using neutron occuring earth alkaloid metals, Naturwissenschaften **27**, 11 (1939). 10.1007/BF01488241

[2] L. Meitner, O. Frisch, Disintegration of uranium by neutrons - a new type of nuclear reaction, Nature **143**, 239 (1939). 10.1038/143239a0

[3] A.V. Karpov, A. Kelić, K.H. Schmidt, On the topographical properties of fission barriers, **35**, 035104 (2008). 10.1088/0954-3899/35/3/035104

[4] A.C. Berriman, D.J. Hinde, D.Y. Jeung, M. Dasgupta, H. Haba, T. Tanaka, K. Banerjee, T. Banerjee, L.T. Bezzina, J. Buete et al., Energy dependence of $p$ +$^{232}$ Th fission mass distributions: Mass-asymmetric standard i and standard ii modes, and multichance fission, Phys. Rev. C **105**, 064614 (2022). 10.1103/PhysRevC.105.064614

[5] J.C. Mein, D.J. Hinde, M. Dasgupta, J.R. Leigh, J.O. Newton, H. Timmers, Precise fission fragment anisotropies for the $^{12}$C + $^{232}$Th reaction: Supporting the nuclear orientation dependence of quasifission, Phys. Rev. C **55**, R995 (1997). 10.1103/PhysRevC.55.R995

[6] E. Williams, D.J. Hinde, M. Dasgupta, R. du Rietz, I.P. Carter, M. Evers, D.H. Luong, S.D. McNeil, D.C. Rafferty, K. Ramachandran et al., Evolution of signatures of quasifission in reactions forming curium, Phys. Rev. C **88**, 034611 (2013). 10.1103/physrevc.88.034611

[7] A.N. Andreyev, J. Elseviers, M. Huyse, P. Van Duppen, S. Antalic, A. Barzakh, N. Bree, T.E. Cocolios, V.F. Comas, J. Diriken et al., New type of asymmetric fission in proton-rich nuclei, **105**, 252502 (2010). 10.1103/PhysRevLett.105.252502

[8] E. Prasad, D.J. Hinde, K. Ramachandran, E. Williams, M. Dasgupta, I.P. Carter, K.J. Cook,

D.Y. Jeung, D.H. Luong, S. McNeil et al., Observation of mass-asymmetric fission of mercury nuclei in heavy ion fusion, Physical Review C **91**, 064605 (2015). 10.1103/PhysRevC.91.064605

[9] C. Bockstiegel, S. Steinhauser, K.H. Schmidt, H.G. Clerc, A. Grewe, A. Heinz, M. de Jong, A. Junghans, J. Muller, B. Voss, Nuclear-fission studies with relativistic secondary beams: Analysis of fission channels, Nuclear Physics A **802**, 12 (2008). 10.1016/j.nuclphysa.2008.01.012

[10] M. Itkis, V. Okolovich, G. Smirenkin, Symmetric and asymmetric fission of nuclei lighter than radium, Nuclear Physics A **502**, C243 (1989). 10.1016/0375-9474(89)90665-9

[11] B.M.A. Swinton-Bland, M.A. Stoyer, A.C. Berriman, D.J. Hinde, C. Simenel, J. Buete, T. Tanaka, K. Banerjee, L.T. Bezzina, I.P. Carter et al., Mass-asymmetric fission of bi-205(,)207(,)209 at energies close to the fission barrier using proton bombardment of pb-204(,)206(,)208, Physical Review C **102** (2020). 10.1103/PhysRevC.102.054611

[12] A. Chatillon, J. Taieb, H. Alvarez-Pol, L. Audouin, Y. Ayyad, G. Belier, J. Benlliure, G. Boutoux, M. Caamano, E. Casarejos et al., Experimental study of nuclear fission along the thorium isotopic chain: From asymmetric to symmetric fission, Physical Review C **99** (2019). 10.1103/PhysRevC.99.054628

[13] P. Morfouace, J. Taieb, A. Chatillon, L. Audouin, G. Blanchon, R.N. Bernard, N. Dubray, N. Pillet, D. Regnier, H. Alvarez-Pol et al., An asymmetric fission island driven by shell effects in light fragments, **641**, 339 (2025). 10.1038/s41586-025-08882-7

[14] J. Buete, B. Swinton-Bland, D. Hinde, K. Cook, M. Dasgupta, A. Berriman, D. Jeung, K. Banerjee, L. Bezzina, I. Carter et al., Universality of shell effects in fusion-fission mass distributions, **865**, 139459 (2025). https://doi.org/10.1016/j.physletb.2025.139459

[15] K. Nishio, A. Andreyev, R. Chapman, X. Derkx, Ch. E. Düllmann, L. Ghys, F. He$\beta$berger, K. Hirose, H. Ikezoe, J. Khuyagbaatar et al., Excitation energy dependence of fragment-mass distributions from fission of $^{180,190}$Hg formed in fusion reactions of $^{36}$Ar+ $^{144,154}$Sm, Physics Letters B **748**, 89 (2015). 10.1016/j.physletb.2015.06.068

[16] R. du Rietz, E. Williams, D.J. Hinde, M. Dasgupta, M. Evers, C.J. Lin, D.H. Luong, C. Simenel, A. Wakhle, Mapping quasifission characteristics and timescales in heavy element formation reactions, Phys. Rev. C **88**, 054618 (2013). 10.1103/PhysRevC.88.054618

[17] L.T. Bezzina, E.C. Simpson, D.J. Hinde, M. Dasgupta, Observation of suppression of heavy-ion fusion by slow quasifission, **306**, 01029 (2024). 10.1051/epjconf/202430601029

[18] D.J. Hinde, M. Dasgupta, E.C. Simpson, Experimental studies of the competition between fusion and quasifission in the formation of heavy and superheavy nuclei, Progress in Particle and Nuclear Physics **118**, 103856 (2021). 10.1016/j.ppnp.2021.103856

[19] D.J. Hinde, D.Y. Jeung, E. Prasad, A. Wakhle, M. Dasgupta, M. Evers, D.H. Luong, R. du Rietz, C. Simenel, E.C. Simpson et al., Sub-barrier quasifission in heavy element formation reactions with deformed actinide target nuclei, Physical Review C **97**, 024616 (2018). 10.1103/physrevc.97.024616

[20] D.J. Hinde, C.R. Morton, M. Dasgupta, J.R. Leigh, J.C. Mein, H. Timmers, Competition between Fusion-Fission and Quasi-Fission in the Reaction $^{28}$Si + $^{208}$Pb, Nucl. Phys. A **592**, 271 (1995). 10.1016/0375-9474(95)00306-L

[21] D.J. Hinde, D. Hilscher, H. Rossner, B. Gebauer, M. Lehmann, M. Wilpert, Neutron emission as a probe of fusion-fission and quasifission dynamics, Phys. Rev. C **45**, 1229 (1992). 10.1103/PhysRevC.45.1229

[22] D.J. Hinde, A.C. Berriman, M. Dasgupta, J.R. Leigh, J.C. Mein, C.R. Morton, J.O. Newton, Limiting angular momentum for statistical model description of fission, Phys. Rev. C **60**, 054602 (1999). 10.1103/PhysRevC.60.054602

[23] B.M.A. Swinton-Bland, J. Buete, D.J. Hinde, M. Dasgupta, T. Tanaka, A.C. Berriman, D.Y. Jeung, K. Banerjee, L.T. Bezzina, I.P. Carter et al., Multi-modal mass-asymmetric fission of 178pt from simultaneous mass-kinetic energy fitting, Physics Letters B **837**, 137655 (2023). 10.1016/j.physletb.2022.137655

[24] J. Buete, B. Swinton-Bland, D. Hinde, K. Cook, M. Dasgupta, A. Berriman, D. Jeung, K. Banerjee, L. Bezzina, I. Carter et al., Evolution of shell-driven fission below the actinides, **1063**, 123174 (2025). 10.1016/j.nuclphysa.2025.123174

[25] G. Scamps, C. Simenel, Impact of pear-shaped fission fragments on mass-asymmetric fission in actinides, Nature **564**, 382 (2018). 10.1038/s41586-018-0780-0

[26] G. Scamps, C. Simenel, Effect of shell structure on the fission of sub-lead nuclei, Physical Review C **100** (2019). 10.1103/physrevc.100.041602

[27] E. Prasad, D.J. Hinde, M. Dasgupta, D.Y. Jeung, A.C. Berriman, B.M.A. Swinton-Bland, C. Simenel, E.C. Simpson, R. Bernard, E. Williams et al., Systematics of the mass-asymmetric fission of excited nuclei from $^{176}$Os to $^{206}$Pb, Physics Letters B **811**, 135941 (2020). https://doi.org/10.1016/j.physletb.2020.135941

[28] V.E. Viola, K. Kwiatkowski, M. Walker, Systematics of fission fragment total kinetic energy release, Phys. Rev. C **31**, 1550 (1985). 10.1103/PhysRevC.31.1550

[29] J. Buete, Australian national university phd thesis: "impact of shell structure on fusion and fission" (2023), http://hdl.handle.net/1885/292208